

Lean Cell Finalization in Lithium-Ion Battery Production: Determining the Required Electrolyte Wetting Degree to Begin the Formation

Jan Hagemeister,* Sandro Stock, Moritz Linke, Marius Fischer, Robin Drees, Michael Kurrat, and Rüdiger Daub

In order to make electric transportation more accessible, the cost of lithium-ion batteries must decrease. One way to achieve this is by increasing the production rates, especially in the time-consuming steps of electrolyte filling and cell formation. Within this work, lithium-ion pouch and hardcase cells are filled with electrolyte and the formation is started at varying wetting degrees. Data from the formation, stabilization, and life cycle testing are analyzed to determine the effect of an incomplete wetting degree on the cell quality. Additionally, postmortem analysis is performed to help understand the mechanisms induced when a cell with incomplete wetting is subjected to a current. The pouch cells demonstrate a linear capacity fade, regardless of the wetting degree, but feature strong lithium plating which becomes visible during postmortem analysis. In contrast, the hardcase cells display a clear correlation between the cell quality and the wetting degree in both the life cycle test and the postmortem analysis. It is shown that a wetting degree of 98% is required before starting the formation to avoid lithium plating in the cell.

1. Introduction

Lithium-ion batteries (LIBs) have never been more in demand than they are today, with production capacities projected to grow exponentially in the coming years.^[1] Especially in the course of climate change, the switch from fossil fuels to renewable energies is becoming inevitable. Energy generation in particular

requires sustainable storage media with LIB as the basis for sustainable mobility.^[2] This high demand makes it necessary to produce LIB even faster. The production steps of LIB exhibit complex interdependencies, which poses a challenge for high-quality and high-throughput cell manufacturing. In this context, the process of electrolyte wetting and subsequent formation are examined, which are located at the end of the production chain and represent a significant bottleneck in battery production due to the long process times of up to 3 weeks.^[3]

The goal of the wetting is to fill every pore with electrolyte liquid, which enables the ionic transport in the cell.^[4] According to Lanz et al., the wetting of LIB has to be completed before starting the formation process.^[5] With completed wetting, the initial charging leads to the formation of the


solid electrolyte interphase (SEI), a passivation layer on the anode active material.^[6] Wetting and formation take 3–7 days, which means that it is a bottleneck in battery production because time and storage capacities are required.^[7] Drees et al. focused on accelerating the formation process.^[8] The authors successfully developed a fast-charging formation procedure that reduced the formation time by over 53% compared to conventional formation procedures. Thus, only 45 min were needed for the formation of the considered cell configuration.^[8]

With the formation times already improving, there remains potential for accelerating the wetting process in order to decrease process times in the cell finalization. Kampker et al. concluded that the wetting of hardcase cells can be accelerated with the use of pressure.^[9] Wood et al. studied the effect of pressure on the wetting process and found that even after 12 and 24 h, there was still a fraction of the pore volume that remained unwetted.^[3] According to Günter et al., the wetting time could be improved from 7.5 h in 2019^[10] to 3 h in 2022^[11] by only changing the process design and parameters. The authors achieved a quicker complete wetting through low pressure at the first dosing step and an overpressure in the second dosing step.^[11]

Kampker et al. explain that a complete wetting is essential to ensure a safe and proper functioning of the battery cells.^[9] Kwade et al. support this statement but elaborate that an unfinished wetting requires multiple formation cycles in order to fully develop

J. Hagemeister, S. Stock, M. Linke, M. Fischer, R. Daub
Institute for Machine Tools and Industrial Management
Technical University of Munich (TUM)
85748 Garching, Germany
E-mail: jan.hagemeister@iwb.tum.de

R. Drees, M. Kurrat
elenia Institute for High Voltage Technology and Power Systems
Technische Universität Braunschweig
38106 Braunschweig, Germany

 The ORCID identification number(s) for the author(s) of this article can be found under <https://doi.org/10.1002/ente.202200686>.

© 2022 The Authors. Energy Technology published by Wiley-VCH GmbH. This is an open access article under the terms of the Creative Commons Attribution-NonCommercial-NoDerivs License, which permits use and distribution in any medium, provided the original work is properly cited, the use is non-commercial and no modifications or adaptations are made.

DOI: 10.1002/ente.202200686

the SEI.^[12] As the SEI can only form on wetted areas, possible results of unwetted areas could indirectly cause harmful anode surface reactions leading to increased aging of the graphite structure.^[13] According to Wood et al., a formation of the SEI is made possible by a complete wetting of the active materials and the separator with electrolyte because this ensures a homogeneous ionic conductivity.^[3] An inhomogeneous formation of the SEI would result in the deposition of lithium, known as lithium plating on the anode. The storage of lithium on the anode results from the fact that the porosity of the anode material decreases due to SEI growth.^[14] Possible effects of an incomplete SEI are also poor cycling tests.^[13] This would cause increased aging, as well as a negative influence on safety. Wang et al. described that an insufficient formation of the SEI leads to a self-amplification of negative effects, which in turn could lead to safety-critical faults.^[15] Hartnig and Schmidt described that with the help of additives, the SEI formation and its properties can be influenced.^[16] Another way of improving the SEI is choosing an electrolyte specially made to enable a longer cycling of the LIB.^[17]

Current quantification methods for the wetting degree of a LIB are electrochemical impedance spectroscopy (EIS) as well as neutron radiography (NR). These two methods are not currently suited for an inline measurement during production because they require additional production steps and do not directly measure the wetting. EIS has been presented as a measurement method for the wetting degree of pouch cells.^[18] Knoche et al. were the first to apply NR in the production of LIBs.^[19] In their work, besides the visualization of the electrolyte filling process, the development of gas on the graphite electrodes during the charging process was examined.^[19] It must be mentioned that NR is a method that can only provide information about the wetting of a 2D plane. Therefore, no statements can be made about how deeply the electrolyte penetrates the pores and thus the wetting degree since it is not possible to consider the electrode surfaces individually.

All cited work about the wetting behavior of LIB concludes that the wetting has to be completed so that the cell quality is not impaired. As there are currently no exact measurement techniques that can be easily implemented into the production line, the question is raised as to when the wetting is complete and the formation can be started without the risk of safety-critical issues. Within this work, a series of pouch and hardcase cells were produced and the formation was started after varying wetting times. Using a combination of cycling data and postmortem analysis, the objective was to find a wetting degree for which the formation could be started without impacting the cycling performance or cell quality, thus decreasing the process time.

2. Experimental Section

2.1. Sample Preparation

The experiments in this work were conducted using two types of cells: pouch cells and hardcase cells. The pouch cells were produced at the Institute for Machine Tools and Industrial Management (*iwb*) of the Technical University of Munich (TUM), while the hardcase cells were produced at the Center for Solar Energy and Hydrogen Research (ZSW) in Ulm. Both

Table 1. Properties of the electrolyte liquid LP572 for surface tension, contact angle, and density with values for thickness and porosity of the Celgard 2325 separator.

Material properties		
Electrolyte	Density [ρ]	1197.6 kg m ⁻³
Electrolyte/separator	Surface tension [σ]	34.61 mN m ⁻¹ [27]
	Contact angle [θ]	45.4°[27]
Separator	Thickness t	25 μ m[28]
	Porosity [Φ]	39–41%[28]

cell formats were filled with electrolyte liquid in a dry room at TUM, providing a dew point of less than -42 °C. The same separator type and electrolyte were used in the production and filling of both cell types. The separator used was trilayer 2325 (Celgard), which is detailed in **Table 1** along with the electrolyte properties. The electrolyte is a 1 M solution of LiPF₆ in a mixture of ethylene carbonate (EC) and ethyl methyl carbonate (EMC), with a weight ratio EC:EMC of 3:7 with 2 wt% vinylene carbonate (VC) from Gotion Inc.

2.1.1. Pouch Cells

The production of the pouch cells for the experiments in this work was performed on semiautomated machines. The cells consisted of 13 anodes and 12 cathodes. The anodes were composed of 95 wt% graphite (SGL Carbon) with 5 wt% polyvinylidene difluoride (PVDF, Solvay) and 1-methyl-2-pyrrolidone (NMP, Sigma-Aldrich). The cathodes consisted of 96 wt% LiNi_{1/3}Co_{1/3}Mn_{1/3}O₂ (NCM111, Umicore), 2 wt% carbon (C65, Timical). The electrode sheets were separated in a remote laser cutting process. The separator was z-folded between the electrode sheets with the tabs facing opposite directions. Subsequently, the tabs and current collector foils were welded together using ultrasonic welding. The finished cell stack was then packaged into a flexible pouch bag with a deep-drawn pocket where one side was left open for the electrolyte filling. The specifications of the pouch cell components are summarized in **Table 2**.

Table 2. Specifications of the pouch cell electrodes used for the experiments in this work.

Electrodes [pouch cell]	Anode	Cathode
Active material	Graphite	NCM111
Single-sided areal loading per side in mg cm ⁻²	7.3	14.4
Single-sided density in g cm ⁻³	1.3	3.0
Porosity in %	32.1	32.2
Foil thickness in μ m	10 (Cu)	20 (Al)
Length in mm	104	101
Width in mm	76	73

Table 3. Specifications of the electrodes of the PHEV1 cells.

Electrodes [hardcase]	Anode	Cathode
Active material	Graphite	NCM622
Single-sided loading per side in mg cm^{-2}	8.6	14.5
Single-sided density in g cm^{-3}	1.4	3.0
Porosity in %	39.5	32.0
Foil thickness in μm	10 (Cu)	20 (Al)
Length in mm	4085	3785
Width in mm	147.7	138.6

2.1.2. Hardcase Cells

The plug-in hybrid electric vehicle (PHEV) cell according to DIN 91252,^[20] known shorthand as PHEV1, had a flat-wound cell assembly with $\text{LiNi}_{3/5}\text{Co}_{1/5}\text{Mn}_{1/5}\text{O}_2$ (NMC 622, BASF) as cathode active material and surface modified graphite SMG-A5 (Hitachi Chemical) as anode active material, as detailed in Table 3.

A different cathode active material was chosen compared to the NMC111 used in the pouch cells to provide insights across various material systems. The electrodes were coated on a double-sided coating line through a slotted nozzle. During the coating process, the atmosphere was controlled at 35% relative humidity. After the coating, the electrodes were calendered to achieve the desired densities and porosities as listed in Table 3. In preparation for assembly, the electrodes were dried in a roll-to-roll convection dryer comprising infrared radiation. The electrodes were assembled in a dry room with a dew point of less than -55°C . The flat wound assembly was contacted via ultrasonic welding, compressed, and inserted horizontally into the hardcase housing together with a spacer. Finally, the lid was welded on top of the casing. For further details about the production processes and their parameters, the works of Günter et al. can be referenced for the pouch^[21] and the hardcase^[10] cells.

2.2. Filling Process

2.2.1. Pouch Cells

The pouch cells were filled with electrolyte in a dry room at TUM. A stationary semiautomatic filling machine (Manz Automation AG) was used. The machine was equipped with a dosing drive of the type Dosino 800 (Metrohm). First, a cell was fitted manually in a workpiece carrier and positioned to allow the injection nozzle to enter the cell. Following, the filling chamber and the cell were evacuated to a pressure of 5 mbar. To provide an inert environment, both the chamber and the cell were purged with a shielding gas (nitrogen) up to a pressure level of 500 mbar. Subsequently, an evacuation to 5 mbar was performed to improve the wetting behavior of the cell. The dosing of the electrolyte was conducted beginning at a cell pressure of 50 mbar. The cell was sealed for 3 s with a sealing pressure of 3 bar and a sealing temperature of 195°C at a pressure of 80 mbar. The cell was removed from the workpiece carrier of the filling machine and connected to the EIS measurement device.

2.2.2. Hardcase Cells

The station for the filling of the hardcase cells was also set up in the dry room at the *iwb* (TUM). The ambient temperature and pressure were 18.2°C and 983 mbar, respectively. The filling machine is a self-developed automatic mobile station equipped with an aluminum vacuum chamber, a MD 4 NT VARIO vacuum pump (Vacuumbrand), solenoid valves (Bürkert), two pressure sensors, and a dosing device.^[11] A vertical filling nozzle was integrated into the vacuum chamber and connected to the dosing unit via a valve. The dosing unit consisted of an interface and a dosing drive of the type Dosino 800 (Metrohm). The cell was fixed in vertical position by a workpiece carrier in the vacuum chamber. The carrier also pressed the hardcase cell against the filling nozzle. A temperature control chamber upstream of the valve ensured the tempering of the electrolyte.

The first step of the filling process was the installation of a cell in the vacuum chamber and the connection with the EIS measurement device. Then, the cell and the chamber were evacuated and purged with nitrogen to decrease the H_2O concentration of the process environment. The filling sequence was initiated by first evacuating to a pressure of 50 mbar. While dosing, the pressure increased to 308 and 1328 mbar during the first and second dosing step, respectively. The electrolyte was tempered to 25°C before each dosing step to keep the electrolyte properties consistent. Synchronized to the start of the first dosing step, the EIS measurement was started. After the second dosing, the cell was closed for wetting. Although different process parameters were chosen for the hardcase cells due to the limited void volume requiring two dosing steps, the electrolyte makeup, electrolyte temperature, and evacuation pressure during the first dosing step were identical for the pouch and the hardcase cells.

2.3. Formation Process and Lifetime Test

After the desired wetting time, the pouch and hardcase cells were removed from the filling station and transferred into the climate chamber for the formation process. To test the quality of the cells, a series of charge and discharge cycles were performed. First, the formation was carried out, which represents the first time that the cells were charged and discharged. Then, stabilization cycles at low C-rates and lifetime tests at higher C-rates were performed. The C-rate is the current at which a cell is charged or discharged in relation to the capacity of the cell. For example, a C-rate of 1 represents a 100% degree of discharge (DOD) within 1 h; a C-rate of 0.5 would be an entire charge or discharge in 2 h. This nomination was used to compare the specific currents at which the cells with different capacities were charged or discharged throughout the experiments.

2.3.1. Formation

In order to investigate the impact of the wetting time for the formation, a fast charging formation protocol was used. The goal of the study was to examine the effect of starting the formation with an uncompleted wetting. If a slow formation of $\text{C}/20$,^[22] for example, had been used, then over the 20 h period all cells would have been completely wetted. A fast formation protocol neglects

the wetting impact during the formation and is more suitable to assess different wetting durations.

Based on the method of Drees et al., the maximum formation current without lithium plating was calculated by means of three-electrode cells in coin cell format (PAT-Cells from EL-Cell).^[8] The fast charging formation strategy was calculated based on an electrode equivalent circuit model which controls the current in order to prevent lithium plating. In a further study, the method was successfully validated by optical postmortem analysis.^[23]

For this study, similar three-electrode cells were assembled and filled with electrolyte in a glove box (LABstar, MBraun GmbH). A Freudenberg FS-5P (Viledon FS 2226 E + Lydall Solupor 5P09B) separator was used which provides excellent electrolyte wettability even without filling at a low ambient pressure level, which is not possible with the used PAT-Cells as they need to be sealed by hand inside the glove box. After 24 h of wetting at 20 °C, the formation of the cells was started using the battery tester (PAT-Tester-x-8, EL-Cell GmbH). The formation current was controlled so that negative potentials of the negative electrode were prevented, which might cause lithium plating. The minimum allowed potential of the negative electrode was set to 20 mV serving as a safety buffer.

As depicted in **Figure 1**, the maximum current was limited to a C-rate of 1.5 C and was downsized to 0.4 C after 68 min for ensuring a minimum negative electrode potential of 20 mV until 80% state of charge (SOC). The maximum current was fixed to 1.5 C as higher currents would not lead to a significantly shorter fast charging time. After performing the test formation to determine the desired current profile, the values were imported to the battery tester (BaSyTec) as a lookup table for the reference formation of both the pouch and hardcase cells.

2.3.2. Stabilization

After the formation, a series 100% DOD cycles at a lower current were performed to complete the SEI formation. A test plan was

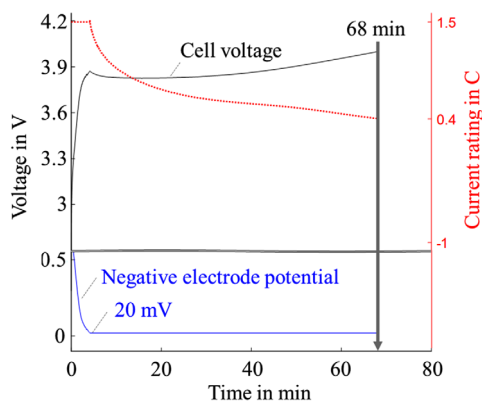


Figure 1. Voltage and current profile of the cell and the negative electrode during charge mode within the fast formation protocol. The formation current was controlled by the negative electrode potential in order to prevent negative electrode potentials below 20 mV which might cause lithium plating. After 68 min, the SOC was 80% which was the end of the charging formation.

used with both a constant current (CC) and constant voltage (CV) mode. First, the cells were discharged at 1 C followed by three charge and discharge cycles. During charging, a current of C/3 was used for the CC phase until the cutoff voltage of 4.2 V was reached. Then, the cell was charged with a CV of 4.2 V until reaching the cutoff current of C/20. The discharging occurred with a CC of C/3 until the lower cutoff voltage of 2.9 V was reached. This sequence of charge and discharge cycle was repeated two times for both cell types. A tabular overview of the test plan for both pouch and hardcase cells is shown in Table A1 and A3, respectively. To analyze the performance of the cells during the stabilization, the coulombic efficiency (CE) is used as a metric. The CE is calculated by dividing the total charge extracted during discharge by the total charge introduced into the cell during the charge cycle.

Gasses which are generated during the SEI formation throughout the formation and stabilization cycles need to be removed from the cell before the life cycle test. The pouch cells were removed from the cell holders and placed into the automated filling and degassing machine. First, the cell was opened to allow the gas to escape from the pouch bag. Then, a vacuum chamber was evacuated to 100 mbar and flushed with nitrogen to 800 mbar for three times before the cell was sealed again. For the hardcase cells, the formation was performed in the dry room with an open cell, allowing the gas to escape continuously. As the stabilization phase took roughly 20 h, the hardcase cells were sealed after the formation to minimize the exposure time to the dry room atmosphere.

2.3.3. Life Cycle Testing

The capacity of the cell used for life cycle testing was determined experimentally by the third discharge cycle of the stabilization. These values were used as the reference for the following life cycle test and are given in Table A2 and A4 of the appendix. Both the pouch and the hardcase cells were cycled in the same temperature chamber used for the formation and stabilization at a temperature of 25 °C. All cells were subjected to two recovery cycles at a low C-rate, followed by 50 cycles at a higher C-rate. These 52 cycles were repeated 19 times for a total of 1040 cycles. For the pouch cells, the first recovery cycle was performed at C/10, the second at C/2, and the 50 cycles at 1 C. The hardcase cells in comparison were subjected to two recovery cycles at C/10 and the 50 cycles at C/2. This was done to highlight the effect of an incomplete wetting degree, without inducing other aging effects in the hardcase cells.

2.3.4. Postmortem Analysis

After the life cycle testing, the cells were opened in a glove box specially designed for postmortem analysis (developed in cooperation with the company MBraun GmbH). The opening was performed in an argon atmosphere (H_2O and $\text{O}_2 < 0.1$ parts per million [ppm]) with constant monitoring of the cell temperature using a thermal imaging camera. Images were taken of the cell components, with focus on the effect of a decreased wetting time on the anode quality.

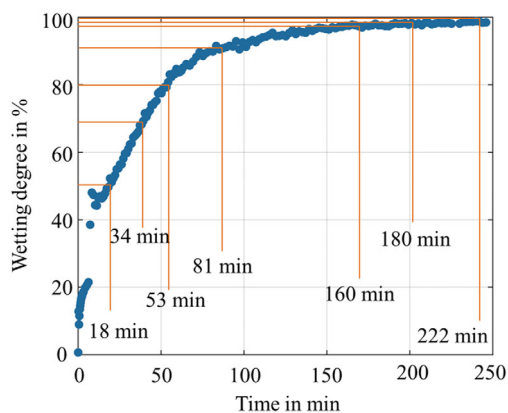


Figure 2. Course of the wetting degree for a PHEV 1 hardcase cell with fixed process parameters. Target wetting degrees were chosen and the respective wetting times were identified for the experiments.

2.4. Design of Experiments

The goal of the experiments was to study the effect of starting the formation before all areas of the cell have been wetted. Shown in **Figure 2** is the course of the wetting degree for a PHEV1 hardcase cell, based on NR images taken during parameter studies by Günter et al.^[11] The wetting degree is the ratio of area filled with electrolyte to the total area of the cell stack, which in this case was defined by the grayscale images of the NR. The cells used as a reference from Günter et al.^[11] had the same cell specifications as the ones used in this work. Additionally, identical process parameters were applied for the reference process and each filled hardcase cell with a pressure tolerance of ± 5 mbar. Although it is not possible to determine the exact wetting degree of each tested cell due to limitations in nondestructive measurement methods, the reproducibility of the wetting behavior of the studied process parameters was shown by Günter et al.^[11] Therefore, it was assumed that all cells exhibit a similar wetting progression. Using this process, target wetting degrees were chosen and the respective wetting times were determined, as shown in **Figure 2**.

An overview of the chosen wetting degrees and wetting times is shown in **Table 4**. Due to the limited void volume, 18 min was the minimum time to complete both dosing steps, which represents a wetting degree of 50%. This cell is denoted as “18 min” in the

Table 4. Target values for the wetting degree corresponding to the wetting times of PHEV 1 hardcase cells.

Wetting degree [%]	Wetting time [min]
50.0	18
65.0	34
80.0	53
90.0	81
98.0	160
98.3	180
98.6	222

results section. In order to induce a wetting degree below 50%, one cell was initially filled with only 80% of the total electrolyte mass to decrease the wetting rate,^[21] which was designated as “18* min” in the further analysis. The remaining 20% electrolyte was filled in a third dosing step before the stabilization cycling. In total, eight hardcase cells were used for the experiments.

For the pouch cells, a similar method was applied to set up the experiments. As there were no NR images available for the pouch cells, EIS was used to determine when all areas of the electrode had been filled with electrolyte and therefore a complete wetting degree had been reached. According to data from Günter et al. 2019, a complete wetting is achieved after 23 min for the given cell system.^[21] As EIS does not provide a progression of the wetting degree, only the final value of 23 min was used to set up the experiments. The shortest time achieved was based on the time it took to remove the cell from the filling machine, place it in the cell holder, and connect it to the testing system. This process took 2 min and set the lower time limit of the experiments. The upper limit for the wetting time was set to 20 h, which provides a large safety factor to ensure complete wetting. Intermediate wetting times of 10 and 40 min were chosen to fill in the range of the five pouch cells shown in the results.

3. Results and Discussion

3.1. Formation

During the formation, the current was controlled by a predetermined profile, as explained in Section 2.3. The theoretical initial capacities for the pouch and hardcase cells were assumed to be 3.25 and 22.00 Ah, respectively. The voltage response to the applied current indicates the charging behavior of the cell. By comparing different voltage profiles, the intercalation characteristics and overpotentials can be observed.^[24] The current and voltage profiles of the pouch and hardcase cells are shown in **Figure 3**.

For the pouch cells shown in **Figure 3a**, the cells with a wetting time ranging from 10 min to 20 h display a very similar voltage development. Within the first 5 min, the voltage rises to just under 3.9 V, and begins to decrease slightly. The first 5 min of the formation is when the cell is subjected to the highest current (1.5 C). Once the current decreases, the voltage decreases slightly. In comparison to the four cells with the longer wetting times, the cell with a wetting time of 2 min displays a higher voltage throughout the entire formation process. During the initial 1.5 C phase, the cell voltage increases to just below 4.0 V and then exhibits a slight decrease, similar to the other cells. The initial voltage spike as well as continuously higher voltage throughout the formation could be an indicator of uneven current distribution due to the uneven ionic conductivity across the electrode surface area. This behavior was especially pronounced in the cell with a wetting time of 2 min, with parts of the electrode theoretically being subjected to over 1.5 C. This could not only lead to a poor SEI formation but also irreversible damage to the electrode surface such as lithium plating at regions with higher current densities.^[8,25] The course of the wetting degree follows an exponentially limited curve, as shown in **Figure 2**. After a wetting time of 2 min, a minority share (<50%) of the electrode had been filled with electrolyte, increasing the current density and leading to

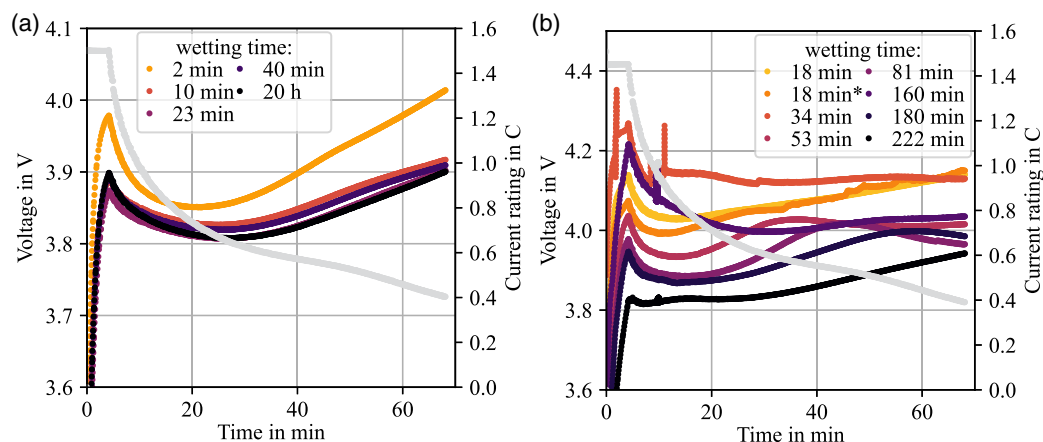


Figure 3. Current rating and voltage data during the fast formation of a) the pouch and b) the hardcase cells after varying wetting times. For each cell type, the current profile is shown on the right y-axis in gray and the resulting voltage profile on the left y-axis. The characteristic increase of the voltage potentials in cells with a shortened wetting time is an indication of inhomogeneous current distributions leading to inhomogeneous SEI formation.

voltage overpotentials. After a wetting time of 10 min, most of the electrode pores were filled with electrolyte such that the current density may be slightly higher ($\approx 10\%$) than with a completely wetted cell but not high enough to cause significant overpotentials.

For the hardcase cells shown in Figure 3b, a similar pattern with a clearer trend is observed. The voltage of the cell with the longest wetting time of 222 min rose to just above 3.8 V, before gradually increasing for the rest of the formation. For cells with decreased wetting times of 180 or 81 min, the initial voltage spike increased to just below 4.0 V. This trend also continued for the wetting times of 53 and 18 min, reaching values between 4.0 and 4.2 V. The cells with a wetting time of 160 and 53 min displayed voltages as well as voltage spikes higher and more inconsistently than the other cells. This behavior is most likely due to contacting issues between the cell and the testing system because due to their high resistances a higher voltage is induced during a set current.

As a conclusion of the formation cycle, it was shown that the pouch cells exhibit very similar behavior for wetting times over 10 min. In the case of a wetting time of 2 min, the voltage was higher than the voltage of the other cells throughout the entire formation, which may be an indicator of higher resistances and irreversible damage to the cell. For the hardcase cells, there is no clear wetting time for which the cells converge toward a particular voltage. The trend shows that shorter wetting times lead to a higher potential during the formation, with two outliers. Additional analysis of the stabilization and life cycle tests were required to better understand the effect of a premature formation, which will be discussed in the following.

3.2. Stabilization

After the formation, a series of charge and discharge cycles were performed to stabilize the cell before the life cycle test, as detailed in Section 2.3. The wetting is expected to progress throughout the cell, regardless of the state of charge so that sufficient wetting can occur during the stabilization. This is supported by the cell capacities after the stabilization, as detailed in Table A2 and A4

of the appendix. **Figure 4** shows the CE throughout the first 11 cycles. The results of the pouch cells shown in Figure 4a demonstrate that the cells with a shorter wetting time exhibit a higher CE during the formation cycle, which is especially evident for a wetting time of 2 min. During the following stabilization cycles at C/3, the cells with shorter wetting times exhibit a lower CE than the cells with a longer wetting time.

This observation is rationalized by considering the current density of cells with varying wetting degrees during the formation. If the wetting degree is incomplete, the entire current distributes among the already wetted region of the cell. The decreased area in which lithium-ion transfer can occur results in a higher current density and thus a higher effective C-rate. The SEI formation is restricted to the wetted regions and lithium plating occurs due to the higher than specified effective C-rate. During the CC discharging, plated lithium in cells with a decreased wetting time will mostly strip and reintercalate into the cathode, resulting in a relatively high discharge capacity which affects the CE. This is due to the energetic benefit of lithium stripping over deintercalation. In a cell with a sufficient wetting time, the SEI will form throughout the entire cell leading to higher irreversible losses due to SEI formation in the first charge cycle with no lithium plating. During the discharging, there is no plated lithium that can be transferred back to the cathode. As the CE is calculated individually for each cell, the effect of varying charge and discharge capacities becomes evident, as shown in Figure 4.

During the following C/3 stabilization cycles, the observation is reversed: cells with a lower wetting time exhibit a lower CE. As the SEI was not able to form in regions without electrolyte during the first formation cycle, it will be compensated during the stabilization cycles. This becomes evident due to a lower CE because SEI losses still occur in comparison to the cells with an already formed SEI from a complete wetting. By the end of the third stabilization cycle, the cells exhibit a similar CE, regardless of the wetting time. This showed that the SEI continues to form throughout the stabilization and it may be feasible to begin the formation in a partial wetting state.

During the third C/3 cycle, the capacity of the cells was on average 3.370 Ah with a slight deviation of 0.025 Ah between

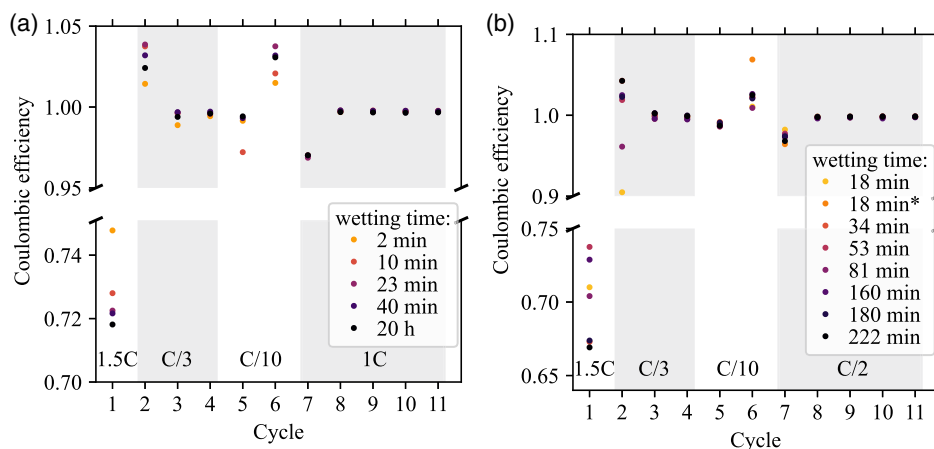


Figure 4. Coulombic efficiencies (CE) during the formation cycle, the three stabilization cycles, the two recovery cycles, and the first five cycles of the life cycle test of a) pouch and b) hardcase cells after varying wetting times. A shortened wetting time leads to a lower CE during the first stabilization cycle but converges with the other cells, demonstrating that the SEI can form even after the initial charging cycle.

the five cells tested. The exact capacity values are provided in Table A2 of the appendix. At each switch of the C-rate, the CE is affected by the previous cycle because there was no CV phase during discharge, which is why the first cycle of a different C-rate is not representative. The first five 1 C cycles demonstrate a similar CE, regardless of the wetting time, demonstrating that the SEI is completely formed throughout the stabilization.

For the hardcase cells shown in Figure 4b, a similar trend is observed compared to the pouch cells: the CE of the cells with a shorter wetting time is higher. The CE during the first stabilization cycle is the lowest for the cell with a wetting time of 18 min, which converges with the other cells during the remaining two stabilization cycles as well as the 1 C cycles. The accelerated fast formation was compensated by the stabilization cycles, which subsequently helped to develop the SEI so that the CE of both the pouch and the hardcase cells was stable during the initial cycles of the life cycle testing.

3.3. Life Cycle Testing

After the formation and stabilization, the cells were subjected to a series of cycles at higher C-rates, as previously detailed. The results of the life cycle test are shown in Figure 5. As a check-up cycle was performed every 50 cycles, the C/10 cycles are shown separately from the 1 C and C/2 cycles for the pouch and hardcase cells, respectively. The normalized discharge capacities were calculated individually for each cell. The measured reference value for the check-up and life cycle is shown in the appendix for pouch and hardcase cells in Table A2 and A4, respectively.

The pouch cells shown in Figure 5a,c exhibit a homogeneous capacity fading over the cycles, with a capacity retention of over 80% throughout 900 cycles at a current rate of 1 C. During the last 200 cycles at 1 C, the cell with the shortest wetting time of 2 min showed a higher capacity retention than all other cells. Based on the data of the five pouch cells, there is no clear effect of a shortened wetting time on the cycling behavior of the cells. The course of the capacity over cycles of each cell has slight fluctuations, but none that indicates a correlation with the wetting

time of the cell, regardless of the C-rate. It could be that for the pouch cells the wetting progressed throughout the 68 min of the formation, such that at the end of the formation the pore volume of the electrodes was filled with electrolyte and could build the SEI. Additionally, the stabilization helped mend any remaining SEI inhomogeneities as displayed by the CE development shown in Section 3.2. Altogether, the lifespan of the pouch cells seems to be unaffected by the wetting time after electrolyte dosing.

For the hardcase cells shown in Figure 5b,d, the life cycle assessment is illustrated separately for the regeneration and the life cycle, similar to the pouch cells. The results show significant differences between the cells depending on the wetting time. For the cells with shorter wetting time between 18 and 53 min, a sharp decline in the capacity retention is shown. While the discharge capacity of these cells during the C/10 cycles is relatively stable, at a C-rate of C/2 strong fluctuations are visible. The cell with a wetting time of 18 min even experienced an internal short circuit and the test was aborted. For the longer wetting times above 81 min, the capacity retention at C/10 is similar to those with shorter wetting times. The difference is evident at the C/2 cycles, where the cells with a wetting time above 81 min (or a wetting degree of 90%) are more stable over the 500 cycles.

In general, a wetting time under 53 min (wetting degree of 80%) is unacceptable for operation because a reliable cell performance cannot be ensured. Slight fluctuations in the discharge capacities could be attributed to the contacting between the cell and the testing system, but the trend prevails that cells with a wetting time of 53 min or below show variations too high for reliable cell performance. Differences due to the wetting degree were shown, with a longer time increasing the cell quality as expected because a complete wetting is conducive for a high cell quality. The sample size for each wetting time was one to minimize the span between data points and to better determine the point at which the formation can begin. This comes at the cost of statistical power because the wetting times were not repeated. Outliers such as the voltage spikes during the formation and mixed cycling data could occur for various reasons as previously discussed, which is why the trends in the data were analyzed in Section 3. Further analysis is required to understand the

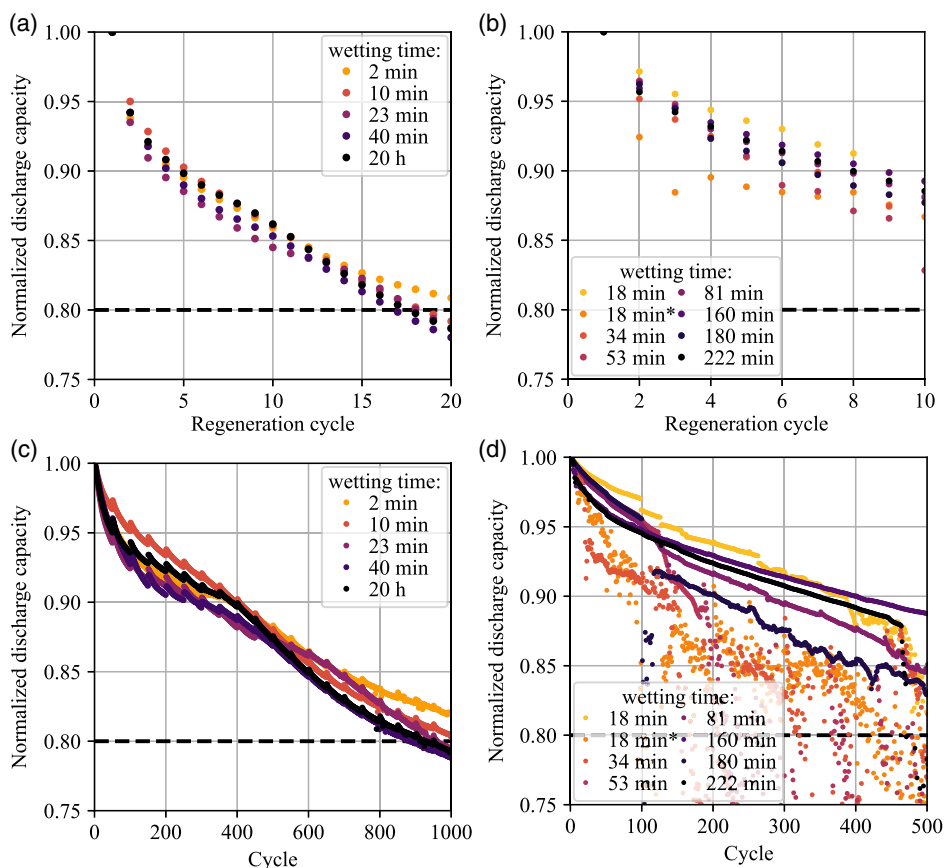


Figure 5. Nominal discharge capacities of a) the check-up and c) the life cycle tests of the pouch cells and b) the check-up and d) the life cycle tests of the hardcase cells. The results of the pouch cells demonstrated an even capacity fade regardless of the wetting time while the hardcase cells with shortened wetting times showed a decreased cycling performance.

predominant mechanisms acting in the cell. For this, postmortem analysis was performed to analyze the electrodes after cycling of the cells.

4. Postmortem Analysis

4.1. Pouch Cells

The postmortem analysis of all five pouch cells was performed after 1000 cycles of life cycle testing at 1 C. Shown in **Figure 6** is the 6th anode sheet of each cell with varying wetting times. The cell with the shortest wetting time of 2 min seen in **Figure 6a** displays a distinct golden mark in the center of the electrode sheet, indicative of lithium plating.^[25] As the electrode separator compound of the pouch cells is a z-folded stack, electrolyte can reach the electrodes from all four edges. This behavior is consistent with NR images published by Günter et al.^[10] and Habedank et al.,^[26] who showed the wetting progression from the outside, resulting in a rectangular shape. This characteristic wetting behavior is consistent with the rectangular golden imprint seen in the center of the electrode shown in **Figure 6**. Also notable are the distinct regions of the lithium plating, which are especially noticeable in **Figure 6a**. One reason for this behavior is the varying wetting rates of the separator, the anode and the cathode,

which induce plating if the lithium ions are unable to intercalate in unwetted regions. Another explanation for the pattern is the wetting state during the course of the formation, such as the beginning and end of the initial charging.

As the wetting time increases in **Figure 6b** or **c**, the mark in the center of the electrode decreases in size while retaining the characteristic pattern of electrolyte wetting. Even after a wetting time of 40 min, the cell still exhibits a small mark in the center of the electrode, although less pronounced than the cell with a wetting time of 10 min for example. After a wetting time of 20 h, it can be assumed that the electrolyte has spread evenly throughout the cell because a wetting period 50 times longer than expected wetting time was chosen. Small marks are still seen, although the plating is most likely not due to the wetting of the cell because the wetting time was so long. It could, for example, be due to gas entrapments during the filling process or plating set on by the 1000 cycles of the life cycle test.

Generally, poor is the occurrence of lithium plating in cells a–d with wetting times up to 40 min. The lithium plating presents a hazard for cell operation as it can induce an internal short circuit within the cell. It is remarkable that although the plating is so pronounced in the postmortem analysis, there was no clear effect in the life cycle test. As a conclusion of the postmortem analysis of the pouch cells, a wetting time under 40 min for the given cell format and configuration is not feasible for cell production

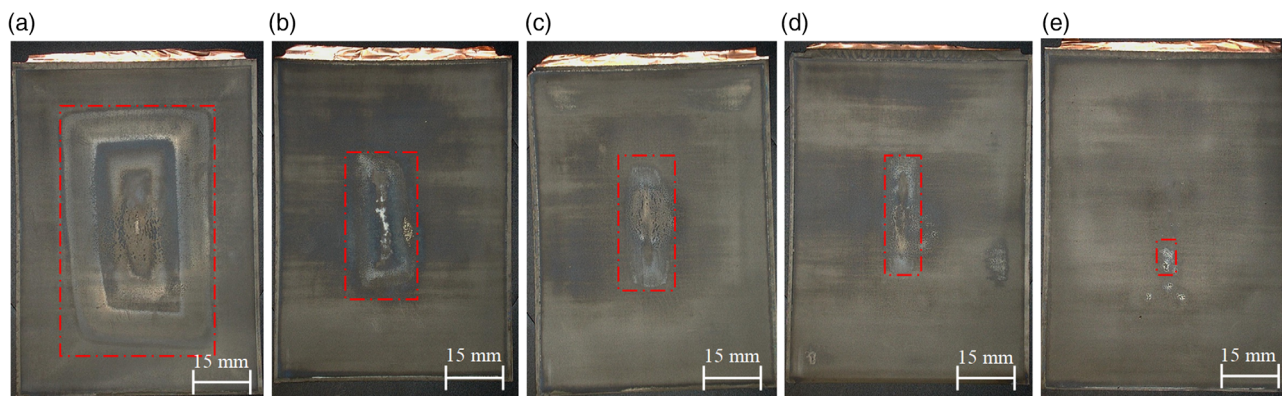


Figure 6. Sixth anode sheet of the pouch cells with wetting times of a) 2 min, b) 10 min, c) 23 min, d) 40 min, and e) 20 h from postmortem analysis. The rectangular golden mark in the center of the electrode, indicating lithium plating as a result of the decreased wetting times, decreases in size with increased wetting times.

due to pronounced lithium plating. Additionally, EIS as a measurement method of the wetting degree needs to be further examined because the cell with a theoretically complete wetting degree after 23 min^[21] showed signs of lithium plating consistent with the pattern of an incomplete wetting degree.

4.2. Hardcase Cells

The hardcase cells were built with a flat wound electrode separator compound, meaning that the electrolyte can only enter the cell stack from only two sides. This means that with a shorter

wetting time, it can be expected that the unwetted center of the cell shows lithium plating. The results of the postmortem analysis of the hardcase cells are shown in **Figure 7**. After a wetting time of 18 min, strong plating is seen in the middle of the electrode. As the wetting time progresses to 34 or 53 min, the area in the middle becomes slightly smaller but keeping the characteristic shape as shown with the red lines. After 81 min of wetting, a small section of plating remains in the center of the electrode, but the overall magnitude of the plating decreases, which can be seen from the decrease in golden marks on the electrode. With a wetting time of 160 min, there are no more marks, same as after a wetting time of 222 min. The cells in

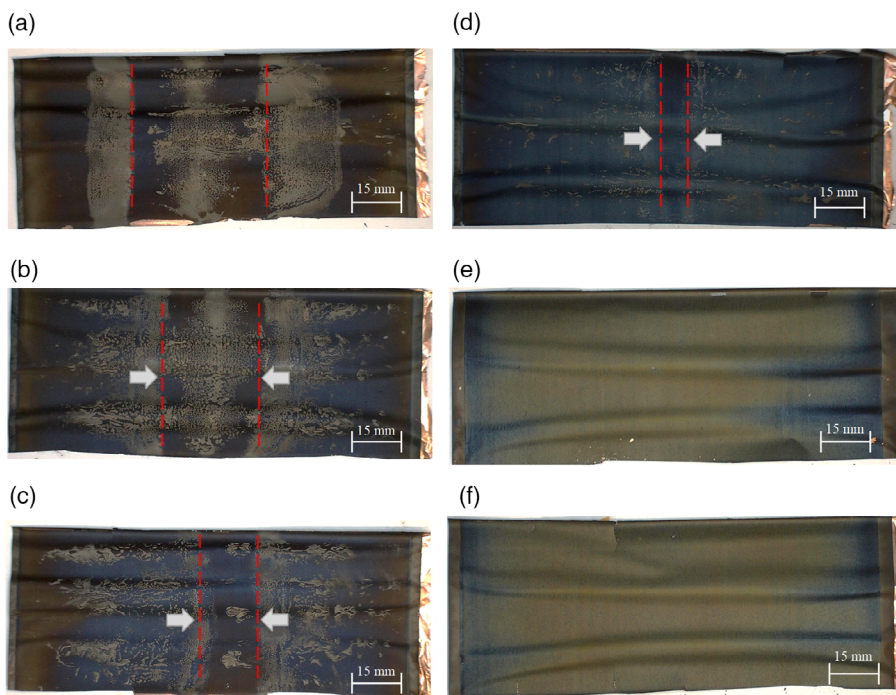


Figure 7. Middle anode section of the hardcase cells with wetting times of a) 18 min, b) 34 min, c) 53 min, d) 81 min, e) 160 min, and f) 222 min from postmortem analysis. The area in the middle of the cell decreases with increasing wetting time, as shown by the red lines. After a wetting time of 160 min, or 98% wetting degree, the lithium plating as a result of an insufficient wetting time has disappeared.

Figure 7e,f show a homogenous anode without any imprint indicative of lithium plating. In each frame, the extent of lithium plating decreases with increasing wetting degrees, as shown by the dashed red lines moving closer together. Even though the sample size of each data point is one, there are no visible outliers in the postmortem analysis, thus reproducibly demonstrating the effects of insufficiently wetted cells during the formation.

As with the pouch cells, any amount of plating is a hazard for the cell operation and must be avoided. The first instance where no plating is evident is after a wetting time of 160 min, which corresponds to a wetting degree of 98% based on NR images. As the cell with a wetting time of 160 min also performed best in the life cycle testing, a wetting degree of 98% would be suitable to begin the formation of a PHEV1 hardcase cell. Compared to a wetting time of 222 min, this represents a 28% decrease in wetting time. As there will always be slight fluctuations in the electrode parameters such as porosity and electrode thickness, as well as process parameters such as pressure and electrolyte quantity, the exact wetting behavior of each cell is unique. Optimizing the process by decreasing the wetting times comes with a risk that must be assessed by each cell manufacturer individually.

5. Conclusion

The goal of the study was to determine if the formation of a LIB can be started prior to a complete wetting. For this, pouch and hardcase cells were produced, filled with electrolyte, and formed after varying wetting times. The results of the pouch cells showed that the CE of the cell with a wetting time of 2 min improved throughout the stabilization cycles, indicating a SEI formation after the initial formation. During the life cycle testing of 1000 cycles at 1 C, all cells performed well with a capacity retention of about 80%, independent of the wetting time. The post-mortem analysis on the other hand showed lithium plating in all cells, with an increasing magnitude as the wetting times decreased. As lithium plating poses a safety hazard, a complete wetting degree is required to avoid risks due to a premature formation.

The hardcase cells showed a similar behavior to the pouch cells regarding the formation and stabilization, but the life cycle tests showed the effect of an incomplete wetting on the cell quality. All cells with a wetting time below 53 min failed during the life cycle testing at C/2, while the cells with longer wetting times maintained a normalized discharge capacity over 80% throughout 500 cycles. The postmortem analysis showed lithium plating in all cells with a wetting degree below 90%, with a pattern characteristic of the wetting progression. After 160 min of wetting, or a 98% wetting degree, there was no more lithium plating visible. This cell also performed best in the life cycle testing, leading to the conclusion that a wetting degree of 98% is sufficient to begin the formation. As no two cells are exactly the same from their electrode pore structure, the wetting times vary between the individual cells. Operating at the limit between process times and cell quality entails a certain risk that needs to be individually assessed by the cell manufacturer. Based on the results shown, starting the formation with an incomplete wetting degree is not recommended.

This work also showcases the value added by performing post-mortem analyses to help understand the aging patterns of the cells. In the case of this study, the cycling data seemed promising for reducing the wetting time, especially in the pouch cells. These findings were contradicted when opening the cells, as lithium plating was visible analogous to the expected wetting behavior. This method of inducing plating by a fast formation of cells with an incomplete wetting degree could also be used to help visualize the wetting behavior of LIB.

As a next step, image processing of the percentage wetting degree shown by the lithium plating during the postmortem analysis could help validate this method of experimental process studies. One approach to quantify the SEI development during the formation is by measuring the gas development, which will be considered in future experiments. Additionally, a 98% wetting degree could be a target value for future experimental and simulation-based process optimization. Measuring the actual wetting degree with advanced methods such as ultrasound could strengthen the results by providing insight into the actual wetting degree in the cell, which will be explored in future work. Combining a fast formation with a shortened wetting time represents the “worst-case scenario” for the cell quality but “best-case scenario” regarding process time. In further studies, the experimental setup could be repeated with a standard formation protocol to investigate the effect of the wetting degree, independent of the fast formation protocol.

Appendix

Table A1. Overview of the testing protocol for the formation, stabilization, and life cycle of the pouch cells. During the formation and the stabilization, the current was identical for all cells, whereas during cycling, the C-rate was determined based on the cell capacity after the stabilization. Data points were recorded every 10 s with $U_{\max} = 4.2$ V and $U_{\min} = 2.9$ V.

Pouch cells					
Procedure	Direction	(Dis)charge	Stop condition	Cycles	Loops
Formation	Charge	Current profile	–	1	1
	Discharge	CC@1C	$U < U_{\min}$		
Stabilization	Charge	CC@C/3	$U > U_{\max}$	3	1
	Charge	CV@ U_{\max}	$I < C/20$		
Cycling	Discharge	CC@C/3	$U < U_{\min}$		
	Charge	CC@C/10	$U > U_{\max}$	–	–
	Charge	CV@ U_{\max}	$I < C/20$	1	–
	Discharge	CC@C/10	$U < U_{\min}$	1	20
	Charge	CC@C/2	$U > U_{\max}$	–	–
	Charge	CV@ U_{\max}	$I < C/20$	1	–
	Discharge	CC@C/2	$U < U_{\min}$	–	–
	Charge	CC@1C	$U > U_{\max}$	–	–
	Charge	CV@ U_{\max}	$I < C/20$	50	–
	Discharge	CC@1C	$U < U_{\min}$	–	–

Table A2. Overview of the cell capacities after the third C/3 stabilization cycle (used for the cell capacities) after the first C/10 check-up cycle and first 1C cycle which were used to calculate the for normalized discharge capacity.

Wetting time	Discharge capacity after third C/3 stabilization [Ah]	Discharge capacity after first C/10 check-up cycle [Ah]	Discharge capacity after first 1C cycle [Ah]
2 min	3.349	3.479	3.259
10 min	3.378	3.497	3.239
23 min	3.392	3.526	3.249
40 min	3.397	3.542	3.273
20 h	3.408	3.550	3.282

Table A3. Overview of the testing protocol for the formation, stabilization, and life cycle of the hardcase cells. During the formation and the stabilization, the current was identical for all cells, whereas during cycling, the C-rate was determined based on the cell capacity after the stabilization. Data points were recorded every 10 s with $U_{max} = 4.2 V$ and $U_{min} = 2.9 V$.

Hardcase cells					
Procedure	Direction	(Dis)charge	Stop condition	Cycles	Loops
Formation	Charge	Current profile	–	1	1
	Discharge	CC@1C	$U < U_{min}$		
Stabilization	Charge	CC@C/3	$U > U_{max}$	3	1
	Charge	CV@ U_{max}	$I < C/20$		
Cycling	Discharge	CC@C/3	$U < U_{min}$		
	Charge	CC@C/10	$U > U_{max}$		20
	Charge	CV@ U_{max}	$I < C/20$	2	
	Discharge	CC@C/10	$U < U_{min}$		
	Charge	CC@C/2	$U > U_{max}$		
	Charge	CV@ U_{max}	$I < C/20$	50	
	Discharge	CC@C/2	$U < U_{min}$		

Table A4. Overview of the cell capacities after the third C/3 stabilization cycle (used for the cell capacities) after the first C/10 check-up cycle and first 1C cycle which were used to calculate the for normalized discharge capacity. The * denotes a modified filling strategy as detailed in Section 2.4.

Wetting time [min]	Discharge capacity after third C/3 stabilization [Ah]	Discharge capacity after first C/10 check-up cycle [Ah]	Discharge capacity after first 1C cycle [Ah]
18	24.196	24.459	23.992
18*	24.011	24.370	23.297
34	24.254	24.626	23.746
53	25.040	25.389	24.676
81	25.302	25.678	24.962
160	24.684	24.845	24.126
180 min	25.290	25.692	24.768
222 min	24.611	24.755	24.165

Acknowledgements

The authors thank the ZSW for the PHEV1 cells and the fruitful discussion especially regarding the execution of the postmortem analysis. The authors also gratefully acknowledge the support from the German Federal Ministry of Education and Research (BMBF) for their financial backing. This work stems from research performed within the scope of the projects Cell-Fill (grant no. 03XP0237B), FormEL (grant no. 03XP0296A), and OptiPro (grant no. 03XP0364B).

Open Access funding enabled and organized by Projekt DEAL.

Conflict of Interest

The authors declare no conflict of interest.

Data Availability Statement

The data that support the findings of this study are available from the corresponding author upon reasonable request.

Keywords

battery production, electrolyte filling, fast formation, lithium-ion cells, postmortem analyses

Received: June 30, 2022
Revised: August 5, 2022
Published online: September 6, 2022

- [1] A. Thielmann, A. Sauer, M. Wietschel, in *Gesamt-Roadmap Lithium-Ionen-Batterien 2030*, Fraunhofer-Institut für System- und Innovationsforschung ISI, Karlsruhe **2015**.
- [2] B. Scrosati, J. Garche, *J. Power Sources* **2010**, *195*, 2419.
- [3] D. L. Wood, J. Li, C. Daniel, *J. Power Sources* **2015**, *275*, 234.
- [4] A. Davoodabadi, C. Jin, D. L. Wood III, T. J. Singler, J. Li, *Extreme Mech. Lett.* **2020**, *40*, 100960.
- [5] M. Lanz, E. Lehmann, R. Imhof, I. Exnar, P. Novák, *J. Power Sources* **2001**, *101*, 177.
- [6] J. Vetter, P. Novák, M. R. Wagner, C. Veit, K.-C. Möller, J. O. Besenhard, M. Winter, M. Wohlfahrt-Mehrens, C. Vogler, A. Hammouche, *J. Power Sources* **2005**, *147*, 269.
- [7] D. L. Wood, J. Li, S. J. An, *Joule* **2019**, *3*, 2884.
- [8] R. Drees, F. Lienesch, M. Kurrat, *J. Energy Storage* **2021**, *36*, 102345.
- [9] A. Kampker, C.-R. Hohenthanner, C. Deutskens, H. H. Heimes, C. Sesterheim, *Handbuch Lithium-Ionen-Batterien* (Ed: R. Korthauer), Springer, Berlin, Heidelberg **2013**, pp. 237–247.
- [10] F. J. Günter, S. Rössler, M. Schulz, W. Braunwarth, R. Gilles, G. Reinhart, *Energy Technol.* **2020**, *8*, 1801108.
- [11] F. J. Günter, J. Keilhofer, C. Rauch, S. Rössler, M. Schulz, W. Braunwarth, R. Gilles, R. Daub, G. Reinhart, *J. Power Sources* **2022**, *517*, 230668.
- [12] A. Kwade, W. Haselrieder, R. Leithoff, A. Modlinger, F. Dietrich, K. Droeder, *Nat. Energy* **2018**, *3*, 290.
- [13] F. German, in *Untersuchungen Zur SEI-Bildung Und Optimierung Der Formation An Lithium-Ionen Voll- Und Halbzellen*, Karlsruher Institut für Technologie (KIT), Karlsruhe **2015**.
- [14] X.-G. Yang, Y. Leng, G. Zhang, S. Ge, C.-Y. Wang, *J. Power Sources* **2017**, *360*, 28.
- [15] A. Wang, S. Kadam, H. Li, S. Shi, Y. Qi, *NPJ Comput. Mater.* **2018**, *4*, 13.
- [16] C. Hartnig, M. Schmidt, in *Handbuch Lithium-Ionen-Batterien*, (Ed: R. Korthauer), Springer, Berlin, Heidelberg, **2013**, pp. 61–77.

- [17] K. Huang, S. Bi, B. Kurt, C. Xu, L. Wu, Z. Li, G. Feng, X. Zhang, *Angew. Chem. Int. Ed Engl.* **2021**, *60*, 19232.
- [18] F. J. Günter, J. B. Habedank, D. Schreiner, T. Neuwirth, R. Gilles, G. Reinhart, *J. Electrochem. Soc.* **2018**, *165*, A3249.
- [19] T. Knoche, V. Zinth, M. Schulz, J. Schnell, R. Gilles, G. Reinhart, *J. Power Sources* **2016**, *331*, 267.
- [20] DIN 91252:2016-11, *Elektrische Straßenfahrzeuge_- Batteriesysteme_- Anforderungen An Die Gestaltung Von Lithium-Ionen-Batteriezellen; Text Deutsch Und Englisch*, Beuth Verlag GmbH, Berlin.
- [21] F. J. Günter, C. Burgstaller, F. Konwitschny, G. Reinhart, *J. Electrochem. Soc.* **2019**, *166*, A1709.
- [22] S. J. An, J. Li, Z. Du, C. Daniel, D. L. Wood, *J. Power Sources* **2017**, *342*, 846.
- [23] R. Drees, F. Lienesch, M. Kurrat, *Batteries* **2022**, *8*, 30.
- [24] Z. Chen, D. L. Danilov, L. H. Raijmakers, K. Chayambuka, M. Jiang, L. Zhou, J. Zhou, R.-A. Eichel, P. H. Notten, *J. Power Sources* **2021**, *509*, 230345.
- [25] M. Ecker, P. Shafei Sabet, D. U. Sauer, *Appl. Energy* **2017**, *206*, 934.
- [26] J. B. Habedank, F. J. Günter, N. Billot, R. Gilles, T. Neuwirth, G. Reinhart, M. F. Zaeh, *Int. J. Adv. Manuf. Technol.* **2019**, *102*, 2769.
- [27] C. Sauter, R. Zahn, V. Wood, *J. Electrochem. Soc.* **2020**, *167*, 100546.
- [28] D. P. Finegan, S. J. Cooper, B. Tjaden, O. O. Taiwo, J. Gelb, G. Hinds, D. J. Brett, P. R. Shearing, *J. Power Sources* **2016**, *333*, 184.